Journal of Polymer Research (2021) 28: 460
https://doi.org/10.1007/s10965-021-02819-0

ORIGINAL PAPER

Synthesis of bi-functional chelating sorbent for recovery of uranium from aqueous solution: sorption, kinetics and reusability studies

Amit Kanjilal[1] · **Krishan Kant Singh**[1,2] · **A. K. Tyagi**[2,3] · **G. R. Dey**[1,2]

Received: 16 August 2021 / Accepted: 4 November 2021 / Published online: 13 November 2021

Abstract

A bi-functional chelating sorbent is synthesised by introducing two different functionalities (amine and amidoxime groups) subsequently on the surface of an earlier synthesized cross-linked poly-acrylonitrile beads. The cross-linked base polymer beads are normally synthesised through suspension polymerisation using acrylonitrile and styrene as monomers and divinyl benzene as cross-linking agent. The bi-functionality is introduced by amination of base polymer in the first step by reacting with diethylenetriamine followed by amidoximation reaction with hydroxylamine hydrochloride in the second step. The incorporation of functional groups on beads are identified and confirmed with FTIR spectroscopy while the surface morphology, porosity and pores dimensions are evaluated by SEM and BET techniques. The saturation sorption capacity of synthesized beads for uranyl ion is tested and found ~ 45 mg g^{-1}, which is significantly higher than the beads functionalized with sole amidoxime group. These bi-functional beads are quite efficient over a wide pH (1–10) range. The kinetics measurements indicate that the synthesized sorbents reach its saturation sorption capacity within 2 h at ~ 25 °C under neutral pH. In this study, the sorbed uranyl ions are eluted out with 1 M HCl efficiently. These beads exhibit excellent reusability up to three cycles without losing much of its capacity, suggesting better usability in real samples.

Keywords Batch adsorption · Cross-linked PAN beads · Bi-functional resin · Diethylenetriamine · Hydroxylamine hydrochloride · Uranyl ion

Introduction

Uranium, an important material is found naturally in terrestrial rocks and soil in very low concentration. It is used as fuel in nuclear reactors either in natural form in Pressurized Heavy Water Reactors or in enriched form in Pressurised Water and Boiling Water Reactors. With gradual increase in the global energy demand and rapidly diminishing fossil fuel reserves, the nuclear energy has evolved as one of the very crucial alternative green sources for power production. With the increase in demand of nuclear energy, it will be quite impossible to keep the supply of uranium fuel intact depending solely upon the sources from terrestrial origins, thus, looking for other alternatives for uranium sources. According to world estimation survey around 4.5 billion tonnes of uranium is available as dissolved salt in seawater [1]. Thus the extraction of uranium from seawater has emerged as an important and thrust area of research in last few decades. Apart from the use as nuclear fuel, depleted uranium is used to make equipment for having very good shielding capability. Moreover, uranium and its compounds are highly toxic, from biological, chemical and radiological perspectives [2, 3]. Hence, the recovery and/or separation of uranium from biological, environmental and radioactive wastes are undoubtedly significant.

Several undesirable water-soluble materials (such as dye, toxic metals and harmful chemicals) present in low

✉ G. R. Dey
grdey@barc.gov.in

Amit Kanjilal
amitkl@barc.gov.in

Krishan Kant Singh
krish@barc.gov.in

A. K. Tyagi
aktyagi@barc.gov.in

[1] Radiation and Photochemistry Division, Bhabha Atomic Research Centre, Trombay, Mumbai 400085, India

[2] Homi Bhabha National Institute, Anushaktinagar, Mumbai 400094, India

[3] Chemistry Group, Bhabha Atomic Research Centre, Trombay, Mumbai 400085, India

concentration are normally removed by using functionalized adsorbents selectively [4–6]. These removal and recovery processes relate to actual application. Reports on selective adsorption of uranium from various aqueous sources such as radioactive wastes, industrial wastes, and sea water are available in literature [4–10]. Traditional separation methods for example solvent extraction is not feasible especially in cases where the desirable elements present in very low concentration needing a large volume treatment. In such cases, the macro-porous polymeric sorbents containing various chelating ligands are quite suitable to treat dilute to very dilute uranium containing aqueous waste solutions. Optimum stability of the complex formed between metal ions present in the solution and the chelating functional groups of resin beads is most important criteria for better reusability and higher sorption capacity of the resin beads towards that particular metal ion. The hydrophilicity and physicochemical stability of polymeric material help in long run operation efficiently during sorption–desorption cycles. Many organic and inorganic sorbent materials are used selectively to extract uranium present in aqueous media as uranyl ions (UO_2^{2+}). These materials include anion and cation exchange resins [11], surface modified Amberlite XAD resins [12], silica and activated silica gel [13], controlled pore glasses [14], extractant encapsulated beads [15–17], polyurethane foam [18] and modified poly-acrylonitrile (PAN) fibres [19]. Polymer based resin beads, membranes or gels suitably functionalized with organic chelating functional groups are regularly used for the separation of uranium from multi-components aqueous solution sources such as seawater or radioactive sources generated in nuclear industries. Numerous sorbents have been reported where the incorporation of various functional groups on PAN based matrix was used as efficient route of preparation [20]. Amidoxime functionality is well recognized for its property to extract various toxic and heavy metal ions selectively from various aqueous sources [21]. Polypropylene fabric grafted with amidoximated PAN [22–24] and amidoxime functional groups incorporated on to crosslinked porous polymeric resin beads [4] are reported as efficient adsorbents for recovery of uranium from seawater.

Sorbents with magnetic properties [25] and functionalized silica particles [26] are two important fields in recent advancement on this field. Furthermore, artificially synthesised functionalized hybrid bio materials have emerged as new kind of adsorbent for the removal of uranium [27–29]. Electrochemical approach with functionalized chitosan electrode have also been used to extract uranium from aqueous media [30]. Recently, Alexandratos et al. have employed bi-functional sorbents containing various amines groups along with amidoxime chelating groups for recovery of uranium from seawater [31]. An excellent review explaining various means of uranium recovery from seawater is worth mentioning at this point to know the wide spectrum of updated materials to serve this purpose [32].

In this work, bi-functionalized crosslinked PAN resin beads were synthesised by suspension polymerization followed by functionalization with diethylenetriamine (NH_2-CH_2-CH_2-NH-CH_2-CH_2-NH_2) (DETA) and hydroxylamine hydrochloride ($NH_2OH.HCl$) subsequently. The relative proportion of two functional groups was optimised to achieve maximum efficacy of the beads towards uranium (U) as UO_2^{2+} sorption. The synthesized beads were used to study uranium extraction from simulated aqueous samples. The main objective in this study is to compare the efficiency towards uranium recovery with our synthesized bi-functional beads with the previously synthesized mono-functional beads containing only amidoxime as chelating groups.

Experimental

Materials

Acrylonitrile (AN), hydroxylamine hydrochloride and diethylenetriamine were purchased from SD Fine Chemicals Limited, India. Divinyl benzene (DVB) and styrene were procured from Sigma Aldrich. Uranyl nitrate hexahydrate ($UO_2(NO_3)_2.6H_2O$) was procured from Honeywell Fluka. The other reagents such as calcium carbonate, sodium nitrite, sodium sulphate, gelatin, azobis-isobutyronitrile (AIBN), methanol and toluene were procured from Thomas Baker Chemicals, India. All the above-mentioned chemicals were of AR grade (≥ 99.9%) and used as received. All the simulated solutions were prepared with deionised water having conductivity of ≤ 0.6 µS cm^{-1} obtained from a Millipore-Q water purification system. A stock solution of 2000 ppm (w/v) uranium (U) was prepared using uranyl nitrate hexahydrate, and diluted accordingly as per the requirement during experiments.

Synthesis of base polymer beads

Crosslinked polymeric beads containing AN and styrene as co-monomers and DVB as cross-linker, were synthesised using a traditional suspension polymerization technique [4] with suitable modifications according to our experimental set-up. Suspension polymerization was carried out with AN, styrene and DVB as organic phase while the aqueous phase was prepared by mixing sodium sulphate, calcium carbonate, sodium nitrite and gelatin with deionised water as discussed previously [33]. The synthesized base polymer beads were washed repeatedly with deionised water and dried in hot air oven overnight at 40 °C and the schematic of the entire procedure is shown in Fig. 1. Several batches of trial experiments were carried out to achieve an optimum condition to

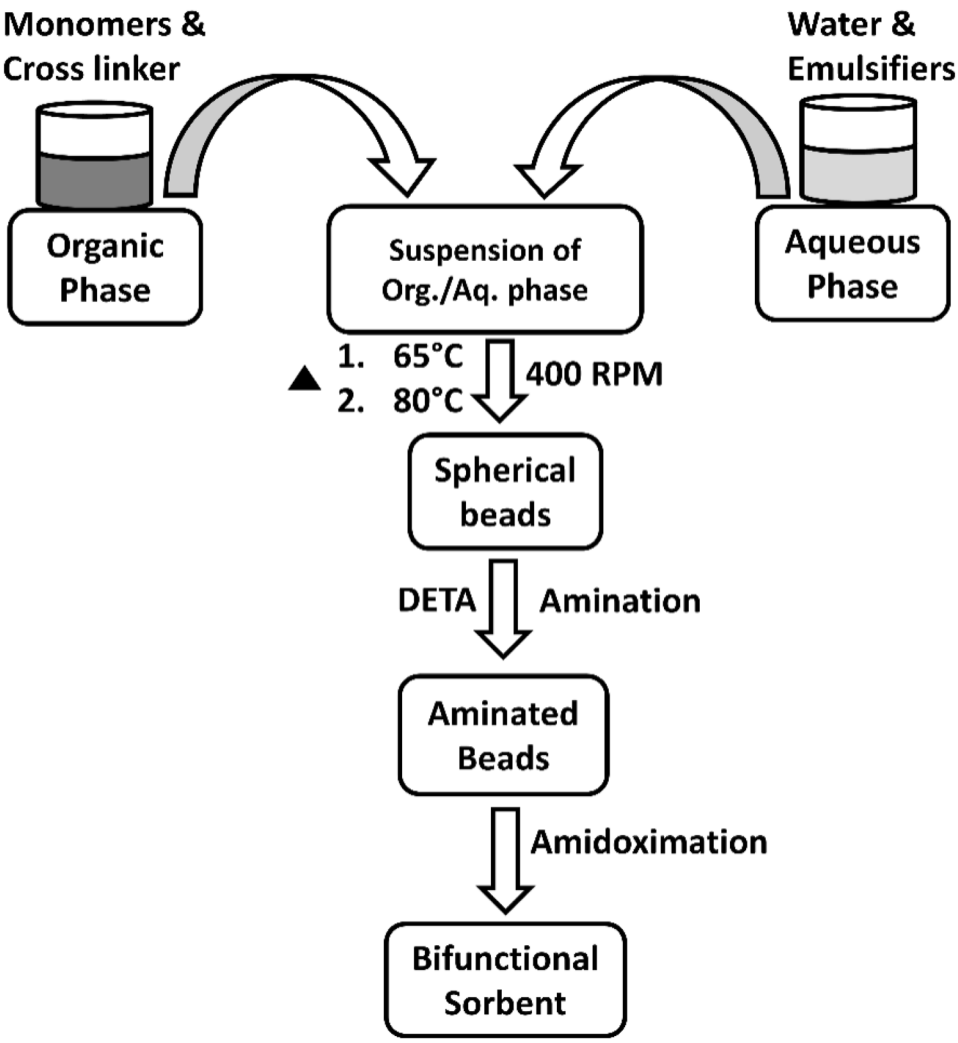

Fig. 1 Schematic presentation of the synthesis process

produce the base polymer beads of desired size and shape. The dried beads obtained were later used for functionalization reactions.

Synthesis of bi-functional chelating resin beads

Bi-functional chelating resin was synthesised in two steps. First, an amine group was introduced by the reaction with DETA followed by amidoximation reaction with hydroxylamine hydrochloride. For amination, 80 ml DETA and 20% sodium carbonate in water (w/v) were mixed in a round bottomed flask. 2 g of dry base polymer beads were added in this mixture and stirred continuously. The whole mixture was kept in stirring condition at 75 °C for 20 h to complete the amination reaction. The initial white coloured base polymer beads became slightly yellowish due to the presence of excess DETA. The beads were washed thoroughly for several times with deionised water to remove excess DETA and sodium carbonate to get back the original white coloured beads and then dried in a hot air oven. The dried beads were weighted to evaluate the % conversion of nitrile (-C≡N) to amine ($-NH_2$) groups.

In the second step of functionalization, amidoximating reagent was prepared by dissolving 4 g hydroxylamine hydrochloride in 1:1 methanol–water mixed solution. The pH of the solution was adjusted to 8.0 with 4 M KOH solution. 2.75 g of dry aminated beads obtained after the first step of functionalization were added to this reagent in a round bottomed flask and refluxed at 80 °C for 2 h for completion of the reaction, which was later verified with FTIR analysis.

Characterisation of synthesized beads

The synthesized bi-functional resin beads were characterised by FTIR spectral measurement with SHIMADZU IR Affinity 1 Spectrophotometer. The shape and size of the synthesised beads were obtained with QX5 Digital Blue Optical Microscope at 60X magnifications. Surface morphology and micro structure of the beads were ascertained by Scanning Electron

Microscope (SEM), using TESCAN VEGA MV 2300 T/A Digital Microscope. The surface area of the synthesised bead was measured by BET surface area analyser. Thermal stability of beads was determined by thermogravimetric analysis (TGA) using METTLER TOLEDO TGA/DSC 1 instrument. The TGA was carried out with few mg of beads sample taken in an alumina crucible at a dynamic temperature range of 25–900 °C at 15 °C min^{-1} heating rate under nitrogen flow (10 ml min^{-1}). All the sorption related studies with UO_2^{2+} solutions were carried out in TARSON ROTOSPIN apparatus at 50 rpm speed.

Sorption of uranium by the synthesized beads

For every sample involving equilibration of the resin beads with aqueous uranium solution, a fixed amount (50 mg) of the synthesised bi-functional beads was added/exposed to 5 ml of UO_2^{2+} solution. After the mixture was equilibrated for a specified period of time under constant rotating condition, the raffinate was analyzed for leftover uranium by ICP-OES. The amount of uranium sorbed on beads was calculated by the difference in concentrations of uranium in the aqueous phase before (C_0) and after (C_e) the equilibration. The amount of uranium sorbed per unit weight of the bi-functional beads at equilibrium (q_e) and the percentage sorption (%A) were calculated using the following expressions:

$$q_e = \frac{\mathrm{v}}{\mathrm{w}} \times C_0 - C_e \tag{1}$$

$$\%A = \frac{(C_0 - C_e)}{C_0} \times 100 \tag{2}$$

where v represents the volume of UO_2^{2+} solution in litres; w is the mass of dry beads in gram and C_0 and C_e are the corresponding initial and equilibrium concentrations of uranium in ppm.

Furthermore, in sorption study, the equilibration with the bi-functional resin beads was carried out for 6 h with the uranyl solutions having uranium concentrations from 10 to 2000 ppm at near neutral pH (~6.8) condition. In kinetics experiment, the resin beads were equilibrated with variable contact time with the uranyl solutions having a fixed uranium concentration (100 ppm). Furthermore, to determine the effect of pH, the sorption experiment was carried out for 6 h fixed contact time with UO_2^{2+} solutions containing 100 ppm uranium at different pHs (ranging between 1 and 13). The aqueous solutions of NaOH and HCl were used to adjust different pHs.

Estimation of uranium

The estimation of uranium in all aqueous samples containing uranium before and after the equilibration with bi-functional resin beads were carried out with inductively coupled plasma-optical emission spectrometry (ICP-OES), using ACTIVA Spectrophotometer from HORIBA JOBIN YVON instrument. ICP-OES suffers from signal suppression and clogging of the nebulizer when the dissolved salt concentration in the sample reaches above 0.2% (w/v) [34], thus proper care was taken on dilution of samples before the analysis. Scott et al. [35] showed that no atomic line of uranium shows any appreciable relative intensity for the determination of uranium by ICP-OES. It was noticed that only the emission from ionic lines was foremost in the spectrum. Thus, the elemental uranium present in solution was analysed by measuring the emission at 385.957 nm wavelength [36]. The relative standard deviation of the instrument while measuring the concentration of uranium in samples was found to be 10%.

Elution and reusability

After the success in uranium (as UO_2^{2+}) sorption by the synthesized bi-functional beads, the studies on elution efficiency were carried out with various acidic reagents such as 0.1 M HCl, 0.1 M HNO_3, 0.1 M Oxalic acid ($H_2C_2O_4$), 1 M HCl, 1 M HNO_3 and 0.5 M H_2SO_4. 50 mg bi-functional beads in six different containers were treated with 100 ppm uranium containing UO_2^{2+} solution separately for 5 h. Concentrations of uranium were analyzed with ICP-OES for each samples and % sorption were calculated following above-mentioned expression 2. After separating out, the treated beads were washed with deionised water, and later equilibrated with 5 ml of each of these six eluting reagents separately. After half an hour of equilibration, the concentrations of uranium in eluting reagents were analyzed. From the measured concentration and the previously calculated % sorption data, the % elution efficiencies were calculated for all six eluting reagents separately. This process was repeated for two more cycles to evaluate the most successful eluting reagent for reusability up to three cycles.

Results and discussion

Synthesis of bi-functional resin beads

Synthesis of bi-functional resin beads was carried out in two steps, synthesis of base polymer beads followed by their functionalization. The first step of beads synthesis is very important for controlling the shape, size, and morphology, which effect directly on stability and reusability of beads in actual application. In conventional suspension polymerisation, several parameters affect the size of polymer beads. Among them the most important are the ratio of organic to aqueous phase and rotation speed of impeller of the reactor.

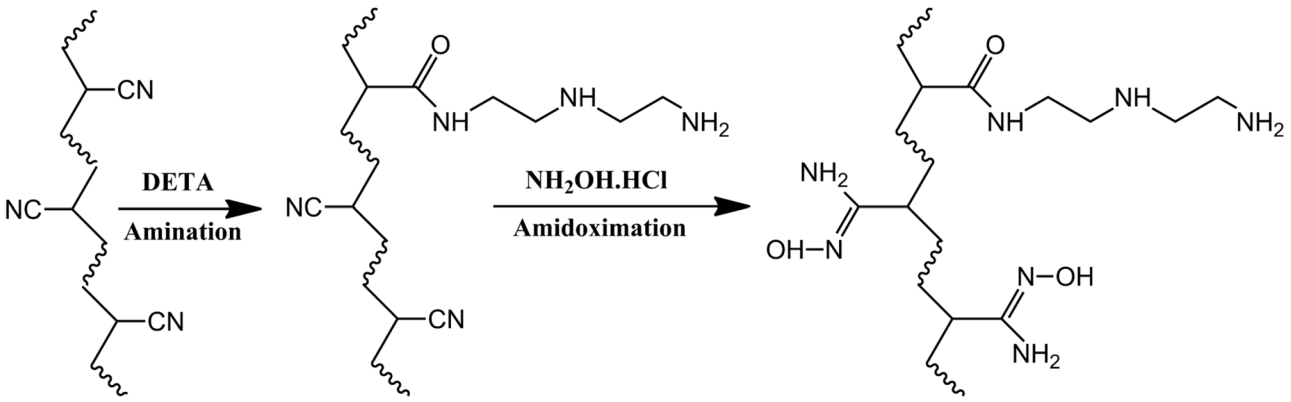

Scheme 1 Stepwise reaction scheme for functionalization

These parameters were carefully controlled to obtain porous base polymer beads of average 300 µm diameter size. The polydispersity index obtained was ~ 20%, which signifies the good uniformity in size distribution of the beads. It is noteworthy to mention here that the incorporation of styrene along with AN as co-monomer helps in formation of beads having higher chemical stability along with good quality spherical shape. This imparts a significant advantage in case of reusability of the beads. The second step in the synthesis includes two consecutive reaction steps to incorporate two different functional groups on the surface of polymer beads. First step is the amination in which DETA moiety is incorporated by reacting with partial free nitrile groups of the base polymer beads with DETA in a control manner so that the remaining nitrile groups can be converted into amidoxime group in the second step of functionalization reaction. This controlled amination was carried out following two simple ways, one by changing the reaction temperature, while the other by varying the duration of amination reaction. The amination process was optimised by varying the reaction duration keeping the temperature constant at 75 °C. It is noteworthy to include that at > 75 °C under the alkaline environment of amination reaction, the physical stability of the functionalized base polymer beads was decreased significantly, which affects the performance and reusability of the beads in long run application. The amination reaction time was varied to 8 h, 16 h, 20 h and 24 h based on the feedback received during several initial studies. After the careful analysis of FTIR spectra for these four aminated polymer beads samples, the materials obtained with 20 h reaction time was selected for further studies. The amidoximation, the second step of bi-functionalization of beads was carried out following the procedure as explained earlier [33]. The reaction scheme of the two steps functionalization is shown in Scheme 1.

Characterization of synthesized beads

The optical microscopy and SEM images obtained with synthesised bi-functional beads are shown in Fig. 2. The diameters of the beads were found within 0.2 to 0.5 mm range

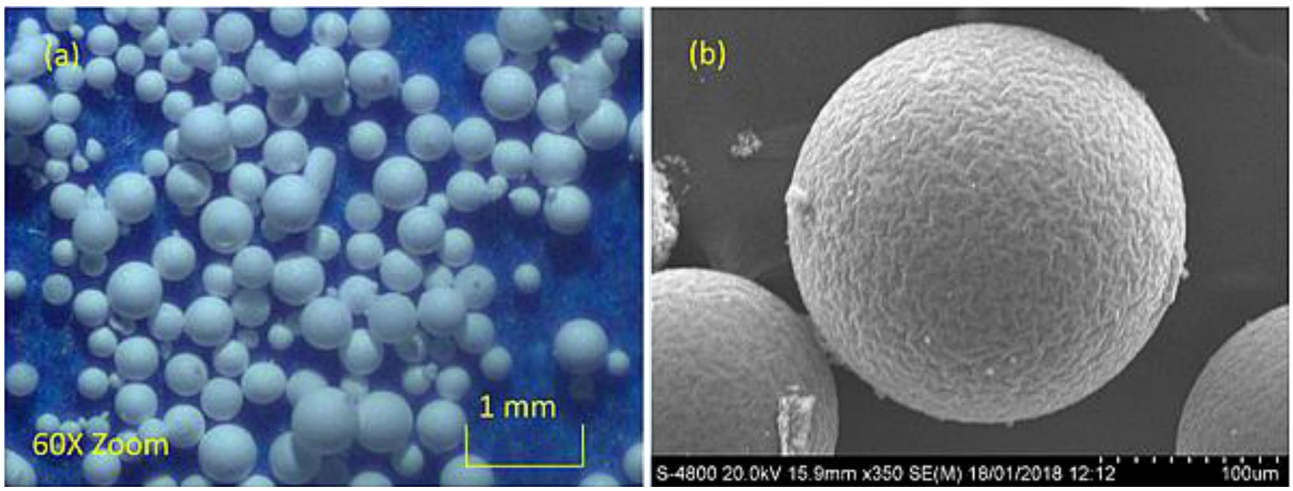

Fig. 2 (**a**) Optical microscopy and (**b**) Scanning electron microscopy (SEM) images of the bi-functional beads

(Fig. 2a). The SEM image (Fig. 2b) exhibits the roughness on resin bead surface that enhances the surface area and perhaps the sorption/desorption of metal ion. Specific surface area of the synthesised beads was found to be ~3.3 m^2/g.

The thermal stability of synthesized bi-functional beads was investigated by thermo-gravimetric-analysis (TGA) in nitrogen atmosphere. The thermograms of bi-functional beads along with the base polymer beads (crosslinked PAN) and beads with only amination are shown in Fig. 3. The loss in weight (~10%) in the temperature range of 25 to 120 °C is because of the moisture content in the mono functional (amine) and bi-functional (amine and amidoxime) beads. Further weight loss (~25%) in 200 to 350 °C temperature range can be attributed to the combined decompositions of amine and amidoxime groups. In addition, the weight loss beyond 400 °C is due to the degradation of the base polymer resin i.e. cross-linked PAN-styrene. In case of only aminated beads, the weight loss occurred in two steps, first one is for amine groups decomposition (~200 °C to ~300 °C) while the other is for base polymer degradation (> 300 °C). The thermogram of the base polymer resin before any functionalization is also compared in the same figure. The one step weight loss starting from ~300 °C suggests the absence of any additional functionality while the sole weight loss can be attributed to the base polymer decomposition. It can also be found that the steps of weight loss in case of the bi-functional beads are not as sharp as that recorded for the base polymer resin, especially from second step of weight loss. This is due to the fact that the degradation of the base polymer starts before the completion of the decomposition of functional groups which causes partial overlap in weight loss steps. The difference in thermogram with bi-functional beads beyond 400 °C is probably associated with the defects occurred in multiple rigorous chemical treatments during two steps functionalization. Especially in case of amidoximation reaction, it was found that the chemical stability of the base polymer reduces with increase in reaction time in a similar type of system [37]. It is noteworthy to include at this juncture that the ratio of two groups i.e. amine/amidoxime is 5:3, which was evaluated from % weight loss in TGA analysis (Fig. 3.)

The FTIR spectra of bi-functional beads along with only aminated beads and base polymer are compared in Fig. 4. The spectrum of base polymer beads showed the prominent peak at 2243 cm^{-1} which corresponds to the free nitrile (-C≡N) groups. Upon amination with DETA the intensity of the said peak was reduced significantly while two new peaks were appeared at 1573 and 1654 cm^{-1}. The peak at 1573 cm^{-1} corresponds to the primary amine group came from DETA while the 1654 cm^{-1} peak is for the C = O stretching vibration of the amide group formed due to the reaction of nitrile with DETA (see Scheme 1). The peaks at 1643 and 911 cm^{-1} observed in the FTIR spectra with

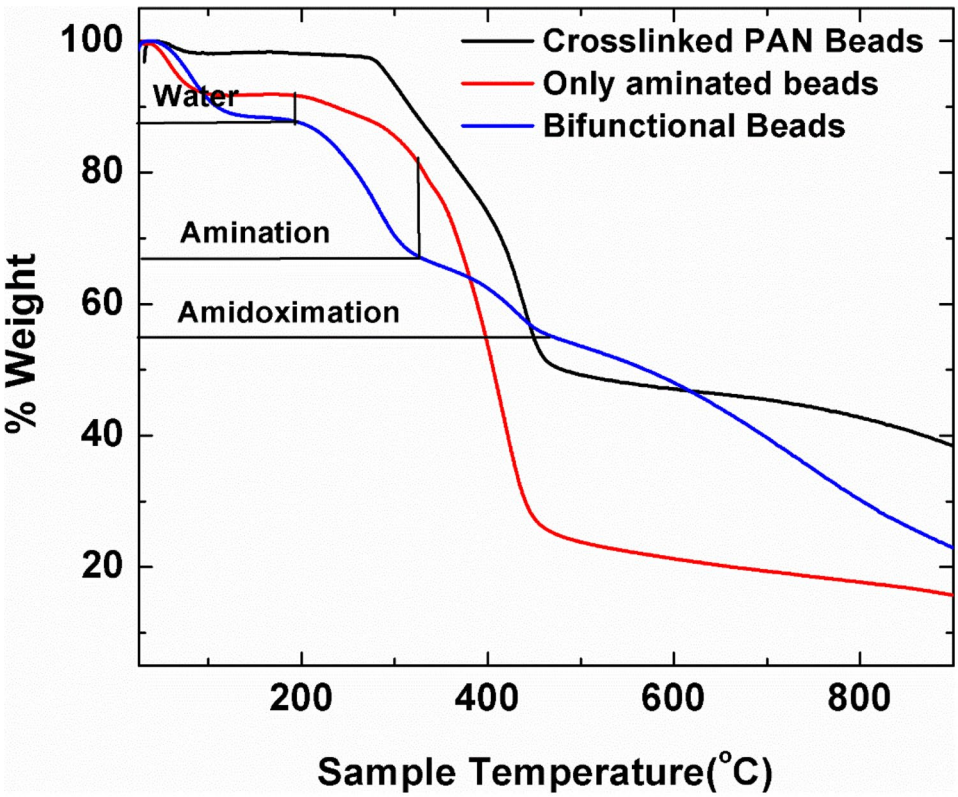

Fig. 3 Thermogramps obtained with bi-functional, aminated resin beads and base polymer in TGA analysis under identical conditions

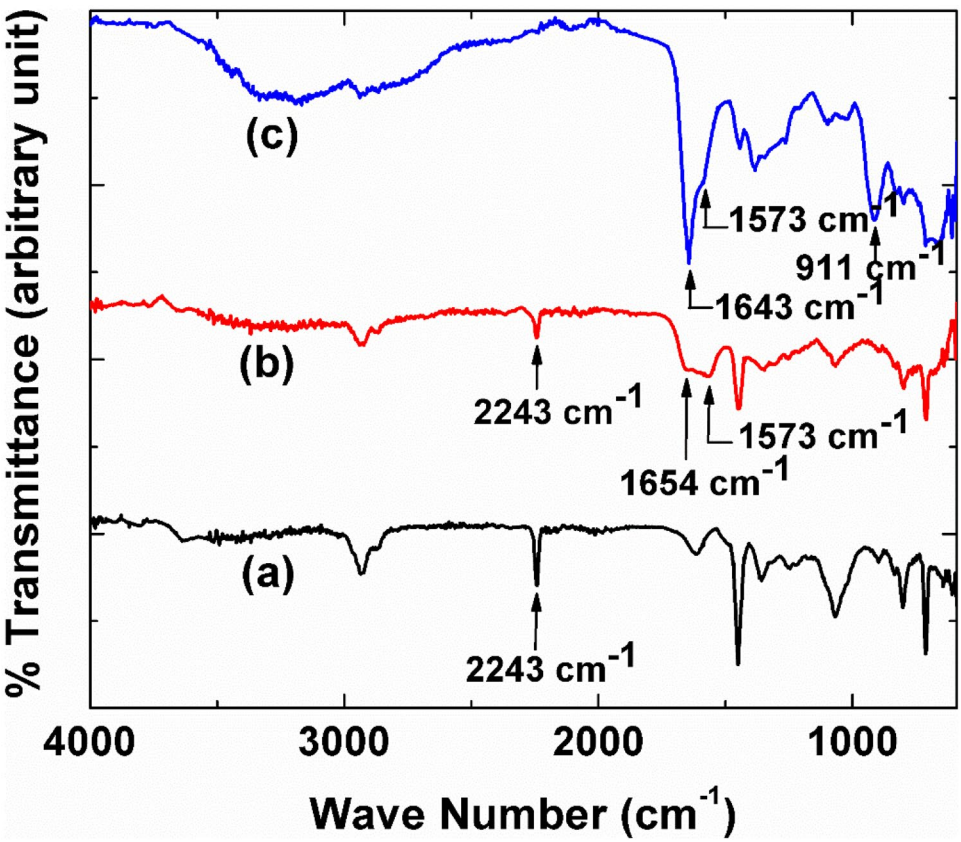

Fig. 4 FTIR spectra in different step of functionalization (**a**) cross-linked PAN beads, (**b**) aminated PAN beads and (**c**) bi-functional beads

bi-functional beads correspond to C = N stretching and N–O stretching vibration of the amidoxime group respectively. Even though the amide vibration is masked under the strong C = N stretching of amidoxime, the 1573 cm^{-1} peak still visible as a small hump in the spectra of bi-functional beads. Along with these peaks, the complete disappearance of the nitrile stretching peak at 2243 cm^{-1} (spectrum C) confirms the total conversion of the nitrile group of base polymer resin to amine and amidoxime. The peaks observed under the band around 2934 cm^{-1} for all three samples are due to C-H stretching available in aliphatic and aromatic site. The broad peak in 3100 to 3500 cm^{-1} region with bi-functional resin also confirms the amidoximation.

Effect of sorption time

The sorption kinetics, a crucial parameter enlightens the efficacy of the sorbent, which is determined by sorption of uptake material (uranium as UO_2^{2+} in this case) by the developed sorbent with respect to contact time that allows the sorbent to adsorb UO_2^{2+}. This study was carried out with the variation of contact time within 5 to 210 min time range at constant temperature (298 K) and pH (pH 6). 50 mg bi-functional beads were added to UO_2^{2+} (equivalent to 100 ppm U) containing solution and the U concentration in solution was analyzed after a particular contact time. This experiment was repeated with the variation of contact time between U solution and bi-functional beads. Figure 5a depicts the uranium sorption capacity with respect to contact/sorption time. It can be seen from the figure that the uptake of U was quite rapid initially up to 10 min, later it slowed down considerably and reached to a steady value at about 2 h, indicating the adsorption/sorption equilibrium point. Therefore, the 2 h contact time was selected for all further experiments to achieve utmost U sorption. In this study the U sorption capacity was found to be 9.5 mg g^{-1}.

Sorption kinetics models

To investigate the mechanism of the sorption kinetics further, the experimental data were ascertained for best agreement with various kinetic models such as pseudo first order, pseudo second order equations and intra-particle diffusion models. Beyond the empirical fitting of the experimental results with various kinetics models, the role of other important phenomenon that can influence the kinetics, such as diffusion, which was taken care in this study [38–44].

For simplicity, we have initiated with pseudo-first-order equation for verification, which is explained below:

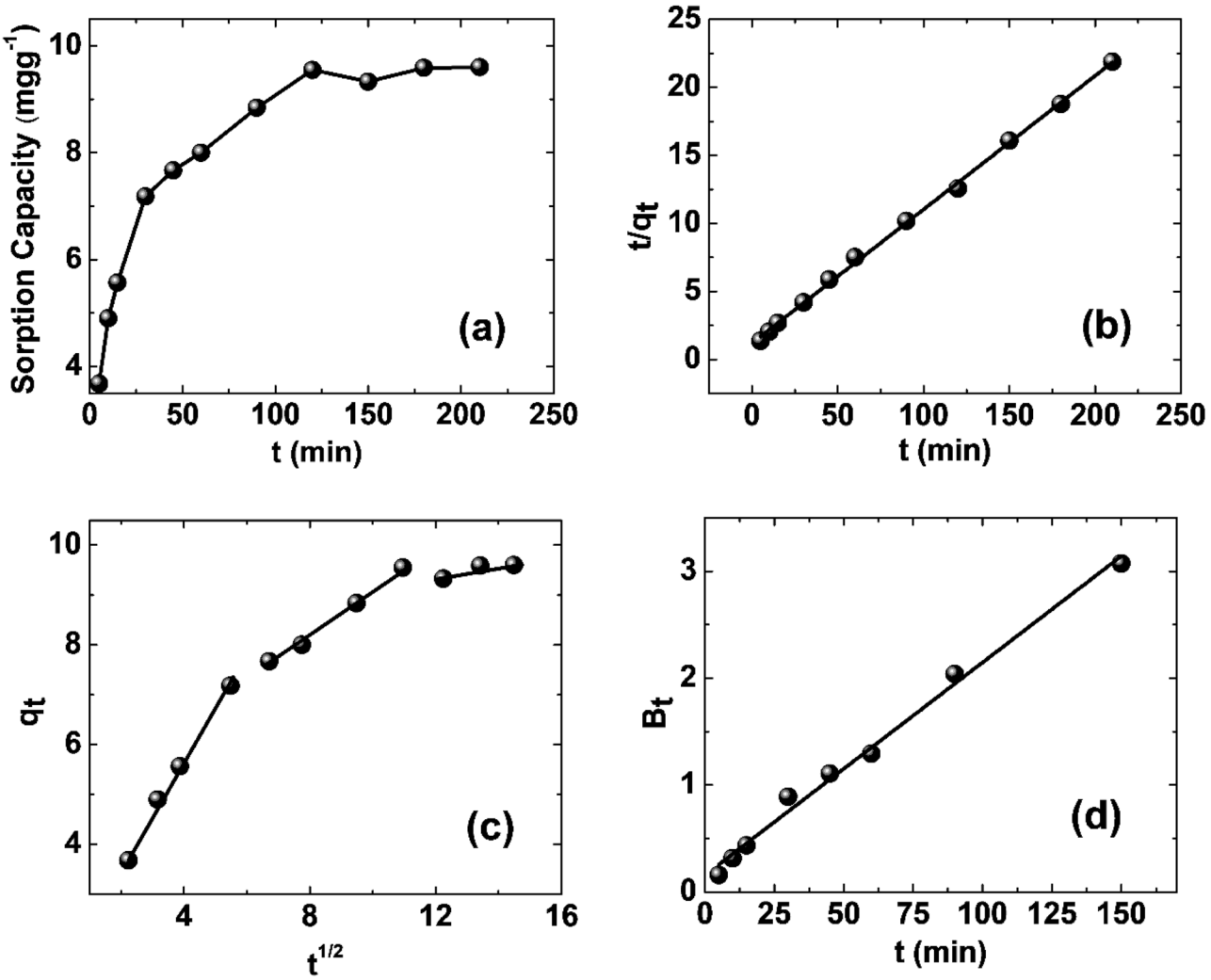

Fig. 5 (**a**) Effect of sorption time; Modelling of kinetics data: (**b**) pseudo second order, (**c**) Intra-particle diffusion, and (**d**) Boyd's plot

Pseudo first-order model

The pseudo-first order model of Lagergren [42] is given as:

$$\frac{dq}{dt} = k_1(q_e - q_t) \tag{3}$$

where q_e and q_t represent the amounts of UO_2^{2+} sorbed on bi-functional beads in mg g^{-1}, at equilibrium and at time t respectively, and k_1 represents the first-order rate constant in min^{-1}.

On integration, the Eq. (3) becomes,

$$\log\left(q_e - q_t\right) = \log q_e - \frac{k_1}{2.303}t \tag{4}$$

The plot of log (q_e—q_t) verses t (not shown) gives correlation coefficient (R_1^2) value of 0.9830 along with k_1 value, which are listed in Table 1. This indicates that the rate of sorption of UO_2^{2+} on bi-functional resin beads was not matched correctly with the experimental data hence the kinetics cannot be explained with the pseudo first-order model. Therefore, the analysis was continued with pseudo-second order model.

Pseudo second-order model

The pseudo-second order model [42] equation is as follows,

$$\frac{dq}{dt} = k_2(q_e - q_t)^2 \tag{5}$$

Where k_2 (g mg^{-1} min^{-1}) represents the rate constant of second-order sorption. The integrated form of the Eq. (5) can be written as,

$$\frac{1}{q_e - q_t} = \frac{1}{q_e} + k_2 t \tag{6}$$

With rearrangement, the Eq. (6) becomes

Table 1 Pseudo-first order, pseudo-second-order and intra-particle diffusion constants and R^2 values for the sorption of uranium onto bi-functional chelating resin beads

U conc 100 ppm	Pseudo first-order			Pseudo second-order			Intra-particle Diffusion			Experimental capacity
	k_1 (min^{-1})	R_1^2	q_e (mg g^{-1})	k^2 (gmg^{-1} min^{-1})	R_2^2	q_e (mg g^{-1})	k_{id} (mgg^{-1} $min^{-1/2}$)	I (mg g^{-1})	R_{id}^2	q_{expt} (mg g^{-1})
	0.0207	0.9830	5.4	0.00809	0.9987	10.17	0.4503	4.586	0.9925	10.04

$$\frac{t}{q_t} = \frac{1}{k_2\, q^2_e} + \frac{1}{q_e} t \tag{7}$$

The plot of t/q_t *vs.* t obtained at pH 6 is shown in Fig. 5b. From the figure, the pseudo-second order rate constant ($k_2 = 8.09 \times 10^{-5}$ g mg^{-1} min^{-1}) and the amounts of uranium sorbed at equilibrium ($q_e = 10.17$ mg g^{-1}) were evaluated from intercept and slope respectively. The obtained correlation coefficients $R_2^2 = 0.9987$ reveals that the sorption kinetics follows the pseudo-second-order kinetic model. It is worth noting at this point that the experimentally U sorption capacity value ($q_{expt} = 10.04$ mg g^{-1}) is very close to the value obtained from pseudo second order model. These results were analysed further utilizing intra-particle diffusion model to understand the diffusion mechanism.

Intra-particle diffusion model

Under this model, the plot of metal ion sorption at various interval of time versus the square root of time decides the contribution of intra-particle diffusion (IPD) in sorption process. If the linear fitting line of the plot passes through the origin then IPD is the rate controlling step [43]. Nevertheless, the plots not passing through the origin is signifying that some degree of boundary layer control, additionally the IPD is not the only rate-limiting step, but other diffusion mechanisms may also take part to control over the rate of sorption, all of which may be operating concurrently.

IPD model is represented as:

$$q_t = k_{id} t^{1/2} + I \tag{8}$$

where k_{id} represents the IPD rate constant and the value 'I' provides the information about the thickness of boundary layer. The IPD plot for the sorption of U on bi-functional chelating beads (Fig. 5c) depicts three linear portions out of which the first two explain the two sorption stages: external mass transfer at initial period followed by IPD of U onto the beads. In the third stage the sorption capacity has become almost independent of time function attaining saturation limit. The slope of the second linear portion gives the IPD rate constant value, which is listed in Table 1.

Boyd's plot

To confirm the sorption process whether it is governed via film diffusion or IPD mechanism, the kinetics data was analysed with expression (9) as given by Boyd et al. [44].

$$F = 1 - \frac{6}{\pi^2} \exp(-B_t) \tag{9}$$

where F represents the fraction of solute sorbed at different time t and B_t represents a mathematical function of F.

$$F = \frac{q_t}{q_e} \tag{10}$$

where q_t and q_e represent the mass of uranium sorbed (mg g^{-1}) at time t and at equilibrium time (120 min in this study) respectively. Depending on the F value, solutions to Eq. (9) are given as Eqs. (11) and (12).

$$B_t = 2\pi - \frac{\pi^2 F}{3} - 2\pi\left(1 - \frac{\pi F}{3}\right)^{1/2} \text{When F } \leq 0.85 \tag{11}$$

$$B_t = -0.4977 - \ln(1 - F) \text{ When F} > 0.85 \tag{12}$$

The B_t values were calculated from the above two equations for different F values and plotted against contact time is shown in Fig. 5d. This figure differentiates between the IPD and the film diffusion mechanism of sorption. A straight line passing through the origin indicates that the sorption processes follows only IPD mechanisms; else, it follows by film diffusion. The linearly fitted Boyd's plot (B_t *vs.* time) does not pass through the origin, signifying that the sorption process is also governed through the external mass transport. Thus, it can be concluded from Fig. 5d that the kinetics of the sorption process is governed by intra-particle diffusion and external mass transport simultaneously.

Sorption isotherm

In sorbent metal ion solution system, the sorption isotherm explains the mathematical relationship between the amounts of sorbent and equilibrium concentration of the metal ion in solution at a constant temperature. To depict the relationship in a graphical manner, the U sorption capacity of the

bi-functional beads was plotted with respect to U concentration and shown as Fig. 6a. This figure depicts that the U sorption capacity increases linearly with the increase in U concentration up to ~500 ppm later it gets saturated gradually with further increase in U concentration. The maximum sorption capacity (q_e) achieved under this condition was ~45 mg g^{-1} in ~1230 ppm U containing UO_2^{2+} solutions, which is quite higher as compared to the beads with only amidoxime functionalized group (~18 mg g^{-1}) under identical experimental conditions [33]. DETA, being a multidentate ligand can form chelating complex with UO_2^{2+} in near neutral pH where amine groups are freely available. This characteristic of DETA may help in enhancing the higher sorption capacity towards UO_2^{2+} along with the formation of stable complex with amidoxime moiety [31].

Initially at lower concentration of UO_2^{2+} the sorption capacity increases almost linearly with the increase in UO_2^{2+} concentration. This clearly indicates that the sorption process in the initial stage is completely dominated by diffusion controlled mass transfer from bulk solution to the surface of the bi-functional beads. However, in later stages the sorption no longer increases proportionately as initial stage with increase in UO_2^{2+} concentration. This probably indicates that the sorption process in greater than 500 ppm U concentration is limited by the number of vacant sites available on the surface of bi-functional beads. Beyond a certain concentration (~1230 ppm) some desorption might be taking place which eventually reduces the sorption capacity marginally.

Sorption results of the bi-functional resin beads with UO_2^{2+} were explored further to verify the sorption isotherm with available models such as Langmuir, Freundlich and Tempkin isotherm models. The details are discussed below:

The Langmuir isotherm model

Langmuir theory of sorption assumes the single monolayer homogeneous adsorption of any adsorbate on the adsorbent's

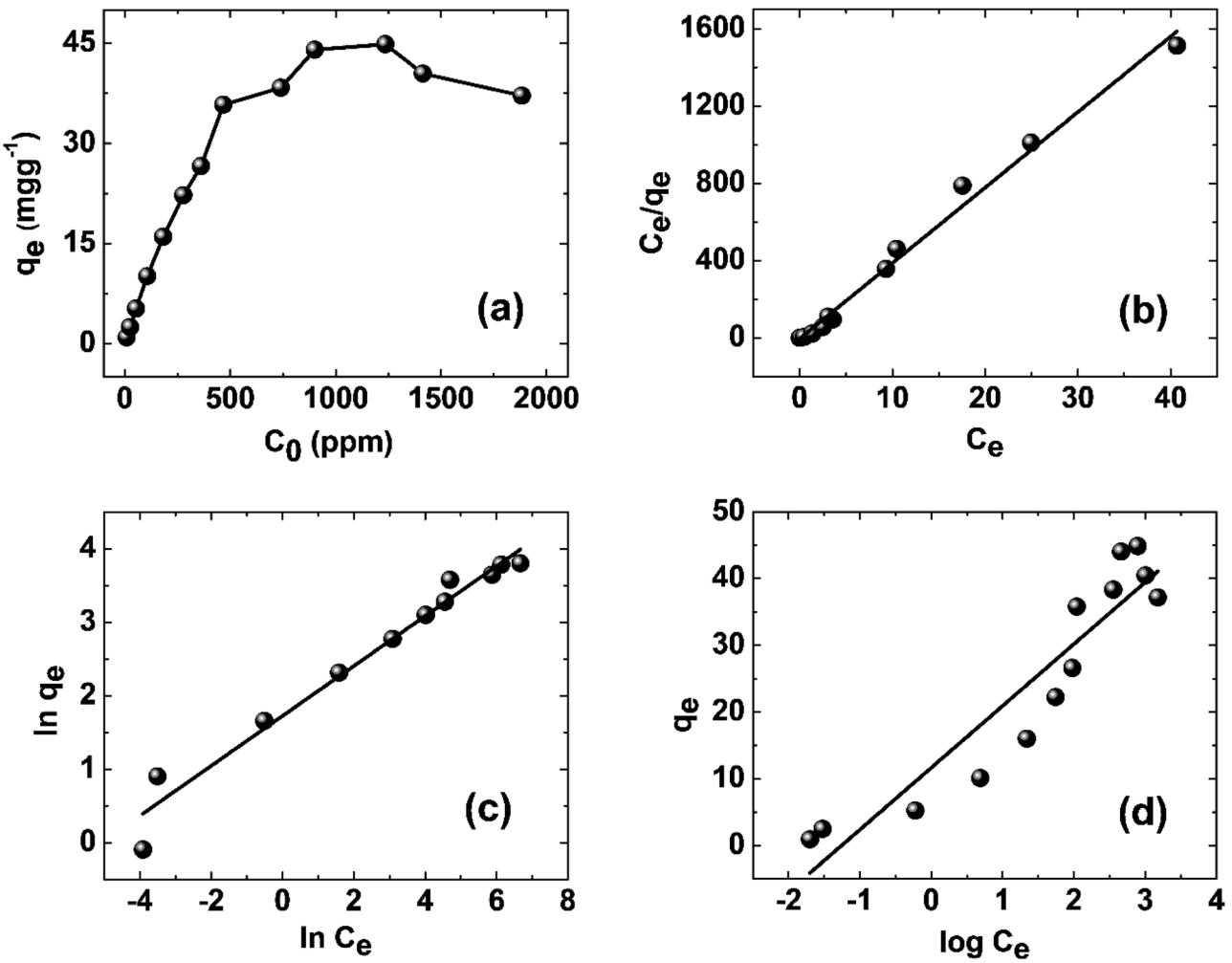

Fig. 6 Modelling of sorption data: (**a**) Sorption of uranium at different concentration, (**b**) Langmuir isotherm, (**c**) Freundlich isotherm, and (**d**) Temkin isotherm

Table 2 Different isotherm constants and corresponding R^2 values for the adsorption of uranium onto bi-functional chelating resin beads

Langmuir Parameter			Freundlich Parameter			Temkin Parameter			Experimental Capacity
q_{max} (mh g^{-1})	b	R^2	k_f (mg g^{-1})	n	R^2	$b \times 10^{-6}$ (J.g.mol^{-2})	A (Lmol^{-1})	R^2	q_{expt} (mg g^{-1})
50.89	0.0027	0.9323	5.6158	2.94	0.9668	166.25	18.06	0.8676	45.18

surface. This means once a site of sorption is occupied by any metal ion (U in this case), there will not be any further sorption possible on to that particular site. The Eq. (13) widely used Langmuir isotherm has been effectively applied in many real sorption processes [45].

$$q_e = q_{max}\left(\frac{bC_e}{1 + bC_e}\right) \tag{13}$$

where, b (L mg^{-1}) represents the Langmuir equilibrium constant, which is related to the affinity of the binding sites, and q_{max} (mg g^{-1}) represents the maximum sorption capacity (theoretical monolayer saturation capacity). The constants b and q_{max}, can be determined from the linearized form of the Langmuir equation, which is given below,

$$\frac{C_e}{q_e} = \frac{1}{(q_{max}b)} + \frac{C_e}{q_{max}} \tag{14}$$

A linear plot of (c_e/q_e) versus c_e (Fig. 6b) having very poor R^2 value (see Table 2) indicates that the sorption behaviour does not follow the Langmuir sorption isotherm. In addition, the maximum U sorption capacity observed experimentally was not matching with the q_{max} calculated through Langmuir model, which pointed out to explore further with other sorption models.

The Freundlich isotherm model

The Freundlich isotherm model is generally used for heterogeneous surface energy systems and for description of multilayer adsorption with interaction between adsorbed molecules. The derivation of the model [46] is given below:

$$q_e = k_f c_e^{1/n} \tag{15}$$

where, constant k_f is maximum sorption capacity associated with the Freundlich isotherm model. The sorption intensity (1/n) describes the linearity of adsorption, which is correlated to the favourability and capacity of the adsorbent/adsorbate system.

To confirm the applicability of the model to the present data, the Eq. (15) can be represented in the following linear form,

$$\log q_e = \log k_f + \frac{1}{n}\log c_e \tag{16}$$

Freundlich isotherm plot obtained (see Fig. 6c) is linear with reasonably good correlation coefficient (R^2) value (0.9668). The evaluated values of k_f and n are also listed in Table 2.

The Temkin isotherm model

This model assumes that the heat due to adsorption of all molecules decreases linearly with the increase in coverage of the adsorbent surface, and that adsorption is characterized by a uniform distribution of binding energies, up to a maximum binding energy. A linearized form of the Temkin isotherm [47] is expressed below:

$$q_e = \left(2.303\frac{RT}{b}\right)\log A + \left(2.303\frac{RT}{b}\right)\log c_e \tag{17}$$

where A represents the equilibrium binding constant (L mol^{-1}) corresponding to maximum binding energy; b is related to the adsorption heat; R represents the universal gas constant (8.314 J K^{-1} mol^{-1}) and T represents the temperature (K). The Eq. (17) can be shortened to Eq. (18), by substituting B for 2.303RT/b.

$$q_e = B\log A + B\log C_e \tag{18}$$

Consequently, the plot of q_e versus $\log C_e$ gives a straight line (see Fig. 6d), using the slope and intercept values, the values of B, A and the correlation coefficient were evaluated, which are listed in Table 2.

Comparing the R^2 values in Table 2 for different isotherms, it is understood that the Freundlich isotherm is a better fit for the given sorption process in this study. Langmuir and Temkin isotherms are not fitting correctly under the testing conditions, and hence these are not accepted to describe the sorption isotherm properly.

Effect of pH on sorption

The pH effect on the sorption performance of bi-functionalized beads towards U (as UO_2^{2+}) was studied at a wide pH range between 1 and 13 and the result obtained is shown in Fig. 7. Surprisingly, the extent of sorption of uranium by the bi-functional chelating beads is quite efficient throughout the pH range up to pH 10, beyond which the sorption decreases significantly. The complex formed between UO_2^{2+} and amidoxime group is explained in literature [48]. Our proposition on complex formation between amidoxime along with amine

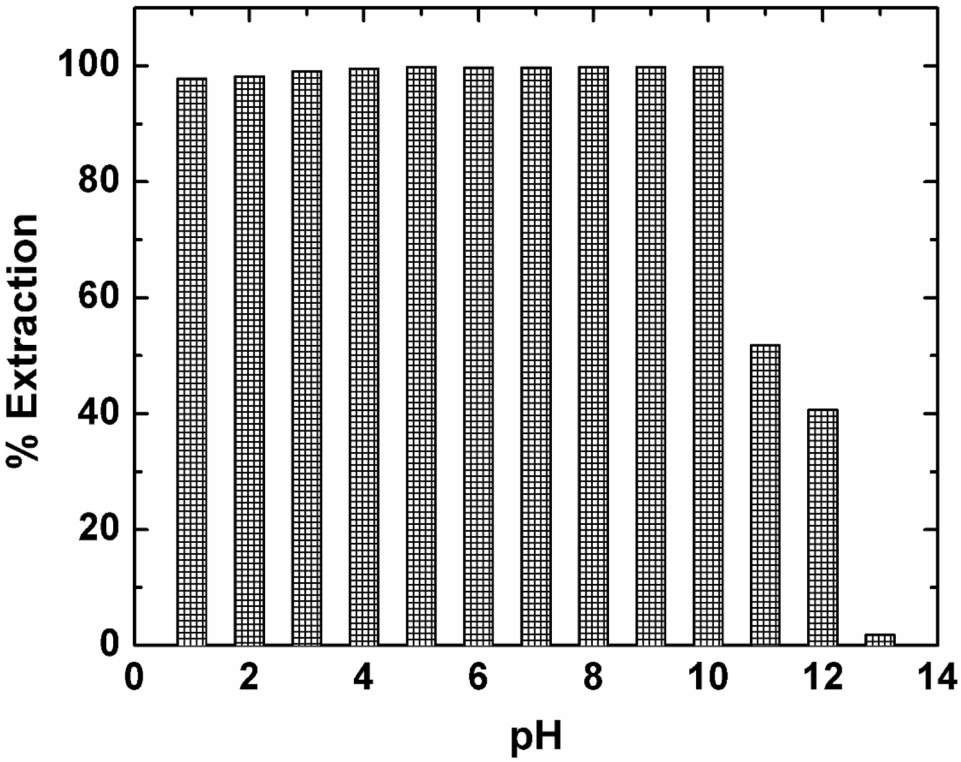

Fig. 7 Effect of pH on sorption of uranium

chelating groups and UO_2^{2+} is shown in Scheme 2. The extent of this complex formation determines the uranium extraction capacity of the synthesized beads under different pH conditions. Two factors are likely to affect the extent of sorption of U under present experimental conditions. First one is the chemical speciation of the UO_2^{2+} present in the medium while the other one is the protonation or deprotonation of the functional groups present on the surface of the resin beads depending on pH of the medium. The pK_a1 and pK_a2 of amidoxime group are 5.78 and 13.21 respectively [49], and the existence of different conjugate forms of amidoxime is shown in Scheme 3.

Below pH 5.78, amidoxime exists predominantly as protonated form (H_2A^+) while above pH 5.78 it exists mainly as free amidoxime (HA). Even though the solubility of UO_2^{2+} in water is quiet high (~120 g/100 g) but it significantly depends on pH of the solvating aqueous medium. This is due to the change in chemical speciation of UO_2^{2+} with change in pH of the medium [50]. As pH of the medium increases, UO_2^{2+} also gradually hydrolyse to $UO_2(OH)^+$ and further to $UO_2(OH)_2$, forming a colloidal precipitate beyond pH 10. Thus in case of only amidoxime functionalized resin beads, due to unavailability of free amidoxime group below pH 5.78, the capacity for uranium sorption remain low at lower pHs (pH < 5) and gradually increases at pH closer to 6. In the present case, the capacity for uranium sorption was found ~90% even at pH 1. This can be explained considering the interplay of the primary amine groups from the

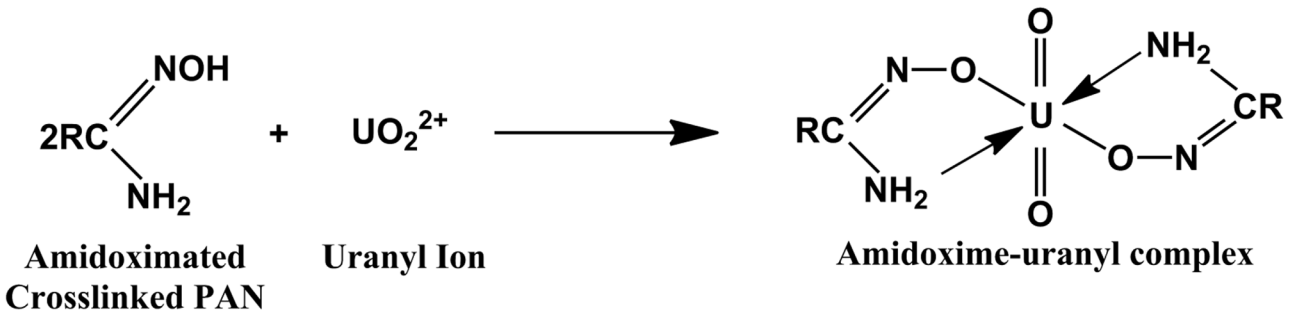

Scheme 2 Complexation of amidoxime with UO_2^{2+} ion

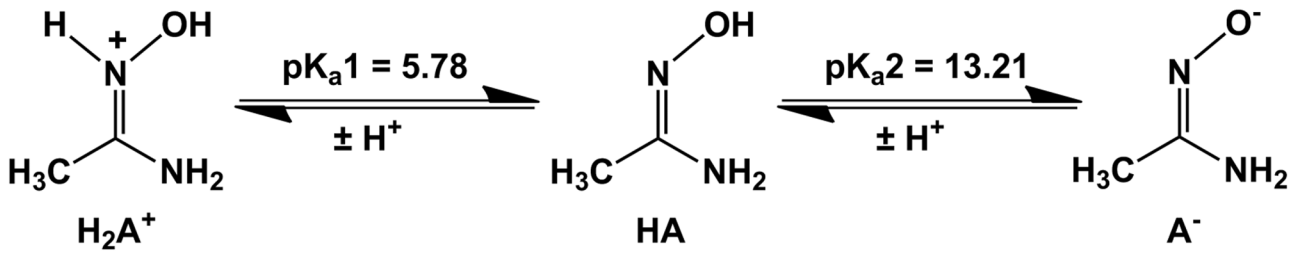

Scheme 3 Different acid–base forms of amidoxime

DETA moiety present on the resin surface with the sorbate ion. As explained elsewhere that the formation of a "pendant complex' of UO_2^{2+} with the primary amine [51] can facilitate the uranium sorption in lower pH which in turn make the sorption capacity as high as 90% even at lower pH values. H^+ ions are very prone to be attached with freely available amine groups. Thus at lower pH, amine groups consume most of the H^+ ions present in the medium leaving the amidoxime groups free which can bind the UO_2^{2+} more efficiently. On the other hand, due to formation of colloidal precipitate $UO_2(OH)_2$, the sorption capacity decreases drastically beyond pH 10.

Elution and reusability

The elution studies with the above mentioned six different acidic eluting reagents were carried out and the result obtained is shown as Fig. 8a, which clearly indicates that 1 M HCl is the most efficient eluting regents among all the reagents used in the experiment. Low acids concentration (0.1 M) was not efficient, which might be due to the fact that the beads have good sorption capacity at lower pH. Thus the strong acidic environment was required to break the stability of the complex of UO_2^{2+} with amidoxime in presence of amine. Even though 0.5 M H_2SO_4 was found efficient for this purpose, but 1 M HCl was chosen for reusability study. This is due to the fact that the PAN based polymeric beads are susceptible to more degradation in sulphuric acid medium in the long run. The reusability study showed very good reproducibility of sorption as well as elution for at least three cycles with 1 M HCl as eluting reagent (Fig. 8b).

At last but not the least, the recovery of uranium from aqueous systems using suitable adsorbents is well known in the area of research and development. There are numerous reports available regarding the efficient recovery of uranium in which various types of materials such as synthetic polymers, carbon based materials, bio sorbents,

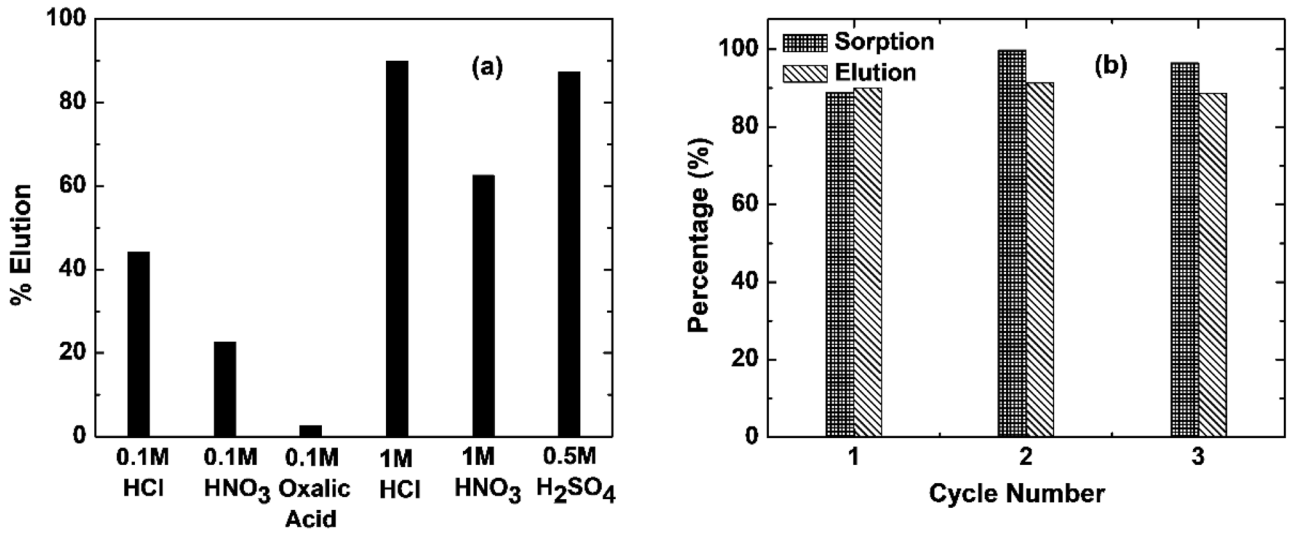

Fig. 8 (**a**) Elution and (**b**) reusability results obtained with bi-functional resin beads

Table 3 Comparison of some selective functional synthetic spherical polymeric sorbents towards uranium sorption

Adsorbent	Uranium Sorption Capacity (mg g^{-1})	Condition of Extraction	Reference
poly(St-co-AO)	0.85	45 ppm uranium, pH 2.2	[54]
poly(AcA-co-MBA)	61.3	1% uranyl solution, pH 8	[55]
poly(AA-co-AcA-co-TMPTA)	250	502 ppm uranium, pH 7	[56]
D2EHPA-Impregnated Polymeric Beads	17	400 ppm, pH 6.8	[16]
2,4-dioxypentan-3-yl methacrylate-coEGDMA IIP	15.3	200 ppm, pH 9, with Na_2CO_3	[57]
Amidoximated PAN-DVB-EGDMA Beads	18.0	400 ppm, pH 6.8	[33]
Bi-functional crosslinked PAN beads	45.0	1232 ppm, pH 6.8	Present Study

polymer composites or new type of porous materials has been employed/developed [52]. Even though the biosorbent materials have inherent advantages of having higher sorption capacity [53] due to the presence of multiple natural hydrophilic functional groups such as -OH and -NH_2, these materials have also limitations in terms of lower reusability while using in multiple cycles along with bio-fouling issue on long run. Synthetic polymers functionalised with different organic groups, is one of the important material with respect to their low cost, reusability and suitability especially in column operation. Table 3 summarises similar functional synthetic co-polymer systems with their uranium uptake capacity along with the respective condition of extraction. Even though some of the sorbent showed better capacity, but if we consider the polymeric beads systems which are easy to use in column mode operation to extract uranium, our bi-functional beads showed reasonably good capacity in a wide range of pH with good reusability admiration. It is noteworthy to mention at this point that with 100 ppm UO_2^{2+} solution the sorption capacity remained almost constant (9.98 mg g^{-1}) within 1–10 pH range. So, this kind of beads has a potential to be used effectively in real condition either in radioactive laboratory or in any natural sources such as uranium contaminated potable water for uranium removal/recovery.

Conclusion

In summary, it was successfully demonstrated that by using synthesized bi-functional (amine and amidoxime) chelating beads, the effective removal of U(VI) ions as UO_2^{2+} is achievable from aqueous solution under batch experimental conditions. The uranium sorption depends on contact time, the initial U concentration and pH. The highest U sorption capacity was found at pH 5.0 which remains steady up to pH 10, later it decreases significantly at above pH 10. The kinetics of sorption/recovery of U was satisfactorily correlated to the pseudo second order kinetic model with further contribution from intra-particle diffusion and film diffusion. Freundlich isotherm model was found to be better correlative with the sorption equilibrium data. The synthesized beads have good capacity for uranium ~ 45 mg g^{-1} uptake as compared to the beads with only amidoxime group (~ 18 mg g^{-1}). The 1 M HCl was found the most efficient eluting agent for the extraction of sorbed U from synthesized beads quantitatively. The extraction performance of bi-functional beads remains similar for three successive cycles of extraction/elution experiments, which reflects its excellent reusability while treating radioactive effluents. This variety of bi-functional beads may serve dual purposes: minimising the health hazard issue due to uranium contamination in ground water and recovery of high-value uranium metal from waste streams.

Acknowledgements This research was carried out under the plan project no: RBA4013. Authors thank the Department of Atomic Energy, Government of India and Bhabha Atomic Research Centre for funding and all the members of Radiation and Photochemistry Division for their support.

Declarations

Conflict of interest No conflict.

References

1. Seko N, Katakai A, Tamada M, Sugo T, Yoshii F (2004) Fine fibrous amidoxime adsorbent synthesized by grafting and uranium adsorption-elution cyclic test with seawater. Sep Sci Technol 39:3753–3767
2. Benedict B, Pigford TH, Lewi HW (1981) Nuclear Chemical Engineering. McGraw-Hill
3. Gadd GM (2000) Bioremedial potential of microbial mechanisms of metal mobilization and immobilization. Curr Opin Biotechnol 11:271–279
4. Egawa H, Kabay N, Shuto T, Jyo A (2003) Recovery of uranium from seawater. XII. Preparation and characterization of lightly crosslinked highly porous chelating resins containing amidoxime groups. J Appl Polym Sci 46:129–142

5. Kabay N, Egawa H (1994) Chelating polymers for recovery of uranium from seawater. Sep Sci Technol 29:135–150
6. Chmielewski AG, Urbański TS, Migdał W (1997) Separation technologies for metals recovery from industrial wastes. Hydrometallurgy 45:333–344
7. Ritcey GM (1980) Crud in solvent extraction processing — a review of causes and treatment. Hydrometallurgy 5:97–107
8. Hudson MJ (1982) An introduction to some aspects of solvent extraction chemistry in hydrometallurgy. Hydrometallurgy 9:149–168
9. Hoh Y-C, Chuang W-Y, Wang W-K (1986) Interfacial tension studies on the extraction of lanthanum by D2EHPA. Hydrometallurgy 15:381–390
10. Tripathi SC, Bindu P, Ramanujam A (2001) Studies on the identification of harmful radiolytic products of 30% TBP-n-dodecane-HNO3 by gas liquid chromatography. i. formation of diluent degradation products and their role in Pu retention behavior. Sep Sci Technol 36:1463–1478
11. Bae SY, Southard GL, Murray GM (1999) Molecularly imprinted ion exchange resin for purification, preconcentration and determination of $UO_2^{2+}$by spectrophotometry and plasma spectrometry. Anal Chim Acta 397:173–181
12. Seyhan S, Merdivan M, Demirel N (2008) Use of o-phenylene dioxydiacetic acid impregnated in Amberlite XAD resin for separation and preconcentration of uranium(VI) and thorium(IV). J Hazard Mater 152:79–84
13. Sadeghi S, Sheikhzadeh E (2009) Solid phase extraction using silica gel modified with murexide for preconcentration of uranium (VI) ions from water samples. J Hazard Mater 163:861–868
14. Northcott SE, Leyden DE (1981) Separation of uranium from molybdenum using a diamine functional group bonded to controlled-pore glass. Anal Chim Acta 126:117–124
15. Girgin S, Acarkan N, Sirkeci AA (2002) The uranium(VI) extraction mechanism of D2EHPA-TOPO from a wet process phosphoric acid. J Radioanal Nucl Chem 251:263–271
16. Singh Krishan K, Pathak Sanjay K, Kumar M, Mahtele AK, Tripathi SC, Bajaj Parma N (2013) Study of uranium sorption using D2EHPA-impregnated polymeric beads. J Appl Polym Sci 130:3355–3364
17. Singh K, Shah C, Dwivedi C, Kumar M, Bajaj Parma N (2012) Study of uranium adsorption using amidoximated polyacrylonitrile-encapsulated macroporous beads. J Appl Polym Sci 127:410–419
18. Toker Y, Eral M, Hicsonmez U (1998) Recovery of uranium from aqueous solutions by trioctylamine impregnated polyurethane foam. Analyst 123:51–53
19. Huang G, Li W, Liu Q, Liu J, Zhang H, Li R, Li Z, Jing X, Wang J (2018) Efficient removal of uranium (VI) from simulated seawater with hyperbranched polyethylenimine (HPEI)-functionalized polyacrylonitrile fibers, New. J Chem 42:168–176
20. Sebesta F, John J, Motl A (1997) Development of composite ion exchangers and their use in treatment of liquid radioactive wastes. International Atomic Energy Agency (IAEA) pp 79–103
21. Omichi H, Katakai A, Sugo T, Okamoto J (1986) A new type of amidoxime-group-containing adsorbent for the recovery of uranium from seawater. II. Effect of grafting of hydrophilic monomers. Sep Sci Technol 21:299–313
22. Kabay N, Katakai A, Sugo T, Egawa H (2003) Preparation of fibrous adsorbents containing amidoxime groups by radiation-induced grafting and application to uranium recovery from sea water. J Appl Polym Sci 49:599–607
23. Prasad TL, Saxena AK, Tewari PK, Sathiyamoorthy D (2009) An engineering scale study on radiation grafting of polymeric adsorbents for recovery of heavy metal ions from seawater. Nucl Eng Technol 41:1101–1108
24. Şahiner N, Pekel N, Güven O (1999) Radiation synthesis, characterization and amidoximation of N-vinyl-2-pyrrolidone/acrylonitrile interpenetrating polymer networks. React Funct Polym 39:139–146
25. Arica MY, Bayramoglu G (2016) Polyaniline coated magnetic carboxymethylcellulose beads for selective removal of uranium ions from aqueous solution. J Radioanal Nucl Chem 310:711–724
26. Bayramoglu G, Arica MY (2016) MCM-41 silica particles grafted with polyacrylonitrile: Modification in to amidoxime and carboxyl groups for enhanced uranium removal from aqueous medium. Microporous Mesoporous Mater 226:117–124
27. Bayramoglu G, Yakup Arica M (2016) Amidoxime functionalized Trametes trogii pellets for removal of uranium(VI) from aqueous medium. J Radioanal Nucl Chem 307:373–384
28. Bayramoglu G, Akbulut A, Arica MY (2015) Study of polyethyleneimine- and amidoxime-functionalized hybrid biomass of Spirulina (Arthrospira) platensis for adsorption of uranium (VI) ion. Environ Sci Pollut Res 22:17998–18010
29. Bayramoglu G, Akbulut A, Acıkgoz-Erkaya I, Arica MY (2018) Uranium sorption by native and nitrilotriacetate-modified Bangia atropurpurea biomass: kinetics and thermodynamics. J Appl Phycol 30:649–661
30. Chi F, Zhang S, Wen J, Xiong J, Hu S (2018) Highly efficient recovery of uranium from seawater using an electrochemical approach. Ind Eng Chem Res 57:8078–8084
31. Alexandratos SD, Zhu X, Florent M, Sellin R (2016) Polymer-supported bifunctional amidoximes for the sorption of uranium from seawater. Ind Eng Chem Res 55:4208–4216
32. Abney CW, Mayes RT, Saito T, Dai S (2017) Materials for the recovery of uranium from seawater. Chem Rev 117:13935–14013
33. Kanjilal A, Singh KK, Bairwa KK, Kumar M (2019) Synthesis and study of optimization of amidoximated PAN-DVB-EGDMA beads for the sorption of uranium from aqueous media. Polym Eng Sci 59:863–872
34. Bahramifar N, Yamini Y (2005) On-line preconcentration of some rare earth elements in water samples using C18-cartridge modified with l-(2-pyridylazo) 2-naphtol (PAN) prior to simultaneous determination by inductively coupled plasma optical emission spectrometry (ICP–OES). Anal Chim Acta 540:325–332
35. Scott RH, Strasheim A, Kokot ML (1976) The determination of uranium in rocks by inductively coupled plasma-optical emission spectrometry. Anal Chim Acta 82:67–77
36. Santos JS, Teixeira LSG, dos Santos WNL, Lemos VA, Godoy JM, Ferreira SLC (2010) Uranium determination using atomic spectrometric techniques: An overview. Anal Chim Acta 674:143–156
37. Shao D, Hou G, Chi F, Lu X, Ren X (2021) Transformation details of poly(acrylonitrile) to poly(amidoxime) during the amidoximation process. RSC Adv 11:1909–1915
38. Brandani S (2021) Kinetics of liquid phase batch adsorption experiments. Adsorption 27:353–368
39. Hubbe MA, Azizian S, Douven S (2019) Implications of apparent pseudo-second-order adsorption kinetics onto cellulosic materials: A review. BioResources 14:7582–7626
40. Hubbe MA (2021) Insisting upon meaningful results from adsorption experiments. Sep Purif Rev. https://doi.org/10.1080/15422119.2021.1888299
41. Tran HN, You SJ, Hosseini-Bandegharaei A, Chao HP (2017) Mistakes and inconsistencies regarding adsorption of contaminants from aqueous solutions: A critical review. Water Res 120:88–116
42. Ho Y, McKay G (1998) A comparison of chemisorption kinetic models applied to pollutant removal on various sorbents, Process Saf. Environ Prot 76:332–340
43. Yang X, Al-Duri B (2005) Kinetic modeling of liquid-phase adsorption of reactive dyes on activated carbon. J Colloid Interface Sci 287:25–34

44. Boyd GE, Adamson AW, Myers LS (1947) The exchange adsorption of ions from aqueous solutions by organic zeolites. II. Kinetics1. J Am Chem Soc 69:2836–2848
45. Langmuir I (1918) The adsorption of gases on plane surfaces of glass, mica and platinum. J Am Chem Soc 40:1361–1403
46. Freundlich HMFZ (1906) Over the adsorption in solution. J Phys Chem 57:385–471
47. Allen SJ, Gan Q, Matthews R, Johnson PA (2003) Comparison of optimised isotherm models for basic dye adsorption by kudzu. Bioresour Technol 88:143–152
48. Vukovic S, Watson LA, Kang SO, Custelcean R, Hay BP (2012) How amidoximate binds the uranyl cation. Inorg Chem 51:3855–3859
49. Mehio N, Lashely MA, Nugent JW, Tucker L, Correia B, Do-Thanh C-L, Dai S, Hancock RD, Bryantsev VS (2015) Acidity of the amidoxime functional group in aqueous solution: A combined experimental and computational study. J Phys Chem B 119:3567–3576
50. Greenwood NNEA (1997) Chemistry of the Elements, Second, Butterworth-Heineman, Oxford
51. Piron E, Domard A (1998) Interaction between chitosan and uranyl ions. Part 2. Mechanism of interaction, Int J Biol Macromol 22:33–40
52. Tang N, Liang J, Niu C, Wang H, Luo Y, Xing W, Ye S, Liang C, Guo H, Guo J, Zhang Y, Zeng G (2020) Amidoxime-based materials for uranium recovery and removal. J Mater Chem A 8:7588–7625
53. Humelnicu D, Dinu MV, Drăgan ES (2011) Adsorption characteristics of UO_2^{2+} and Th^{4+} ions from simulated radioactive solutions onto chitosan/clinoptilolite sorbents. J Hazard Mater 185:447–455
54. Ramachandhran V, Kumar SC, Sudarsanan M (2001) Preparation, characterization, and performance evaluation of styrene-acrylonitrile-amidoxime sorbent for uranium recovery from dilute solutions. J Macromol Sci A 38:1151–1166
55. Pal S, Ramachandhran V, Prabhakar S, Tewari PK, Sudersanan M (2006) Polyhydroxamic acid sorbents for uranium recovery. J Macromol Sci A 43:735–747
56. Chauhan GS, Kumar A (2008) A study in the uranyl ions uptake on acrylic acid and acrylamide copolymeric hydrogels. J Appl Polym Sci 110:3795–3803
57. Zhang H, Liang H, Chen Q, Shen X (2013) Synthesis of a new ionic imprinted polymer for the extraction of uranium from seawater. J Radioanal Nucl Chem 298:1705–1712